

Analysis of π^+p Elastic Scattering from 2.74 to 4.0 GeV/c at All Angles*

Shu-Yuan Chu and Archibald W. Hendry

Physics Department, Indiana University, Bloomington, Indiana 47401

(Received 19 April 1971)

We analyze π^+p elastic scattering in terms of s -channel helicity amplitudes. We demonstrate that the data are consistent at all angles with the picture of scattering from an interaction region of radius 0.8 F, with special edge effects accounting for backward scattering.

I. INTRODUCTION

Recent experiments on the π^+p elastic scattering have provided a new wealth of data for this reaction in the energy range 2.74 to 5.0 GeV/c. Many striking features are to be observed in the data, particularly in the differential cross sections.¹⁻⁴ Near the forward direction, the differential cross section (see Fig. 1) shows a very strong diffraction peak which falls off by two orders of magnitude in the comparatively small interval of momentum transfer $0 \geq t \geq -0.8$ (GeV/c)². Around $t = -0.85$ (GeV/c)², some structure develops - there is a substantial change of slope, with a shallow valley occurring here at the lower energies. The subsequent shoulder then falls off to a very deep valley in the vicinity of $t = -2.8$ (GeV/c)². In the backward direction, there is likewise a sharp peak, followed by a valley which remains at about $u = -0.2$ (GeV/c)² for all the energies considered. At intermediate angles, where the differential cross sections become exceedingly small, there are interesting indications of further structure.

While some of these features have been known for a long time, what is important about the new experiments is that they provide continuous measurements *over the whole scattering region*, and therefore present a challenge to phenomenologists that is considerably more intriguing than the simpler game of fitting *either* the forward *or* the backward scattering data.

There are also some polarization data^{2,5} in this energy range, but these at present cover only the angles near the forward and backward directions. Near the forward direction (see Fig. 2) the polarization is positive, rising initially to about 20-30%. Next, there is a shallow dip around $t = -0.6$ (GeV/c)², after which the polarization increases again to more than 50%. Away from the backward direction (see Fig. 3) the polarization is at first positive (rising to 100% for 2.75 GeV/c), then changes sign at about $u = -0.24$ (GeV/c)², roughly the same position at which the striking backward valley in the differential cross section occurs.

The π^+p total cross section has also been mea-

sured⁶ throughout this energy range (see Fig. 4). It is smoothly decreasing, indicating that there are no really prominent resonances present.

Previous attempts⁷⁻⁹ have been made to fit and understand separate pieces of this data. In particular, the experimental structures at the ends of the angular region are usually interpreted in terms of exchanges in the t and u channels. However, a clear picture of the pion-nucleon interaction from the point of view of these exchanges has yet to emerge, in spite of the enormous effort put into these models during the past decade. Even the basic question of the dip mechanism, whether due to nonsense wrong-signature zeros or to strong pole-cut interference,⁹ is still unresolved.

In the present paper, we suggest another type of model, based on an s -channel approach. This model makes use of the familiar ideas of the optical and absorptive models; however, the present model goes *far beyond* previous models of this type in that it attempts to describe scattering at *all* angles. In a sense, our model can also be regarded as an extension of the more conventional phase-shift analyses¹⁰; however, in order to make the expansions in angular momentum states tractable, we inject some physics (indeed, essentially the same *physics* as went into the original Regge-pole model more than 10 years ago).

In Sec. II we briefly describe the ideas of our model, and in Sec. III we state our parametrization of the amplitudes. In Sec. IV the fits to the data are presented and the contributions from the various amplitudes examined in detail. In Sec. V a brief comparison is made with Regge-pole fits. Finally, in Sec. VI, we discuss the major evidence for our scattering picture.

II. MODEL

The authors have previously outlined some of the basic ideas of the model in their discussion of the π^-p charge-exchange (CEX) reaction.¹¹ There it was shown, through the use of s -channel helicity amplitudes, how the well-known structures in *both* the forward and the backward directions for CEX

could be correlated. (It will be recalled that in the usual Regge approach, these directions are treated totally independently.) The essential points of the argument were the following:

(i) In the angular momentum expansion of the s -channel helicity amplitudes¹²

$$f_{++}^s = \frac{1}{k} \sum_j (j + \frac{1}{2}) T_{++}^j d_{\frac{1}{2}\frac{1}{2}}^j(\theta),$$

$$f_{+-}^s = \frac{1}{k} \sum_j (j + \frac{1}{2}) T_{+-}^j d_{-\frac{1}{2}\frac{1}{2}}^j(\theta),$$

where k is the c.m. momentum, the low-angular-momentum states are absorbed (as a result of S_{e1}^j being small for low j), while the high-angular-momentum states likewise give little contribution since they are unscattered. This leads to the conclusion that the major contribution to the scattering for this CEX process comes from a narrow intermediate band of angular momentum states.

(ii) By considering the oscillations of the corresponding $d_{\lambda\mu}^j(\theta)$ functions, it was shown that this band should be centered around $j = j_c$, where $j_c + \frac{1}{2} = kR$. Here R is the appropriate radius for the interactions, estimated qualitatively to be about 1 F in order to give the forward and backward CEX dips at their observed positions, $t = -0.6$ and $u = -0.2$ (GeV/c)², respectively. As a consequence, we anticipated that if R is more or less a constant, then j_c should move with energy in proportion to the c.m. momentum k .

We now carry over these same ideas to the case of $\pi^+ p$ elastic scattering, one of the few reactions where good data¹⁻⁶ are available at all angles. Elastic scattering has, of course, the added complication of diffraction, and this must be taken into account. The low-angular-momentum states which get absorbed out in many of the inelastic reactions such as CEX are just those which give rise to the strong forward diffraction peak in elastic scattering, analogous to Fraunhofer diffraction in optics. In the present situation, where the proton has spin $\frac{1}{2}$, this effect might be expected to be much more pronounced in the helicity-nonflip amplitude f_{++}^s than in the helicity-flip amplitude f_{+-}^s , which vanishes in the forward direction by angular momentum conservation.

III. PARAMETRIZATION

The parametrization we choose is intended to reflect the physical ideas discussed in Sec. II. We took the angular momentum s -channel helicity amplitudes in the following form:

$$(j + \frac{1}{2}) T_{++}^j = G_{++}^R + iG_{++}^I + \frac{1}{2} \Gamma(v + ix) [(j - j_c) - i\Gamma/2]^{-1},$$

$$(j + \frac{1}{2}) T_{+-}^j = G_{+-}^R + iG_{+-}^I + \frac{1}{2} \Gamma(y + iz) [(j - j_c) - i\Gamma/2]^{-1}. \quad (1)$$

Here G^R , G^I were taken as Gaussians of the form $a \exp[-b(j - c)^2]$. These weight the low angular momentum states (see Fig. 8), in accordance with the relation $T^j = i(1 - S^j)$ and the property that the S -matrix elements for low j are small. It is the Gaussian iG_{++}^I which gives rise to the large forward-diffraction peak; loosely speaking, it corresponds in Regge language to the Pomeranchuk contribution, though, as we shall see later, the contributions of this Gaussian and the Pomeranchukon to the scattering are *markedly different* in detail.

The Breit-Wigner terms are meant to represent the peripheral interaction; that is, the contribution from the band of angular momentum states being scattered from the edge of the absorbing proton target. The choice of a Breit-Wigner form is of course very restrictive. It correlates both the magnitudes and phases of adjacent angular momentum states within this band, and therefore represents some kind of a collective effect. This form also has a certain amount of appeal, however, since it corresponds to a simple Regge pole in the s channel; it is the well-known form which describes grazing rays in classical scattering theory. The parameters j_c and Γ were taken to be the same in both helicity-nonflip and -flip amplitudes.

Therefore, for a given energy in which the dif-

TABLE I. Values of our parameters for fits in Fig. 1. Dimensions of a^R , a^I , v , x , y , and z are $\sqrt{\text{mb}}$ GeV.

| p_{lab} (GeV/c) | | 2.74 | 3.0 | 3.5 | 4.0 |
|--------------------------|---------------------|-------|-------|-------|-------|
| G_{++}^R | a_{++}^R | -0.46 | -0.46 | -0.47 | -0.49 |
| | b_{++}^R | 0.94 | 0.45 | 0.32 | 0.26 |
| | c_{++}^R | 1.88 | 1.64 | 1.72 | 1.90 |
| G_{++}^I | a_{++}^I | 1.16 | 1.22 | 1.21 | 1.28 |
| | b_{++}^I | 0.28 | 0.24 | 0.15 | 0.14 |
| | c_{++}^I | 2.43 | 2.70 | 3.28 | 3.33 |
| G_{+-}^R | a_{+-}^R | | | -0.06 | -0.05 |
| | b_{+-}^R | | | 1.65 | 2.99 |
| | c_{+-}^R | | | 1.05 | 1.54 |
| G_{+-}^I | a_{+-}^I | | | -0.09 | -0.05 |
| | b_{+-}^I | | | 1.01 | 2.50 |
| | c_{+-}^I | | | 1.37 | 0.50 |
| | $j_c + \frac{1}{2}$ | 4.16 | 4.31 | 4.89 | 5.03 |
| | Γ | 0.95 | 0.92 | 0.95 | 0.95 |
| | v | 0.33 | 0.20 | -0.09 | 0.03 |
| | x | 0.31 | 0.28 | 0.15 | 0.16 |
| | y | 0.55 | 0.52 | 0.29 | 0.27 |
| | z | -0.24 | -0.15 | -0.21 | -0.14 |

ferential cross section at all angles, the available polarization, the total cross section, and the ratio of the real to the imaginary part of f_{++}^s at $t=0$ are all fitted simultaneously, there are, all together, 18 parameters. (The two Gaussians in the flip amplitude, however, give fairly small contributions, so that all the basic structures are given, essentially, by 12 parameters.) We also make sure that the parameters change smoothly on going from one energy to the next (see Table I).

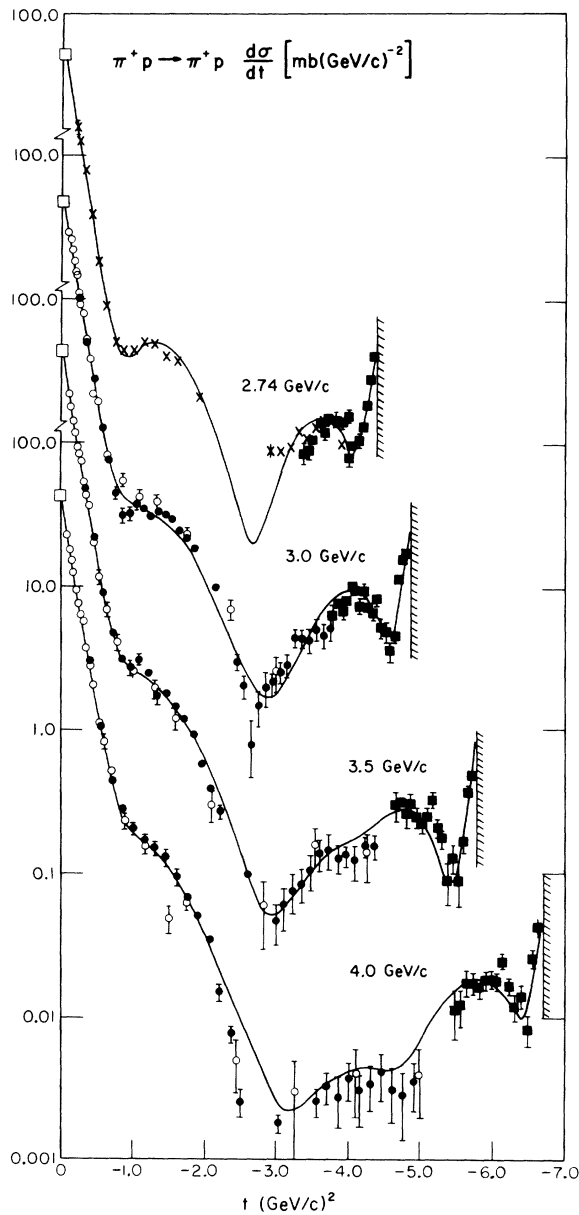


FIG. 1. Fits to π^+p elastic-scattering differential cross section at $p_{lab}=2.74, 3.0, 3.5$ and 4.0 GeV/c. Data from Ref. 1 (●, ■), Ref. 2 (×), Ref. 3 (○), and Ref. 13 (□).

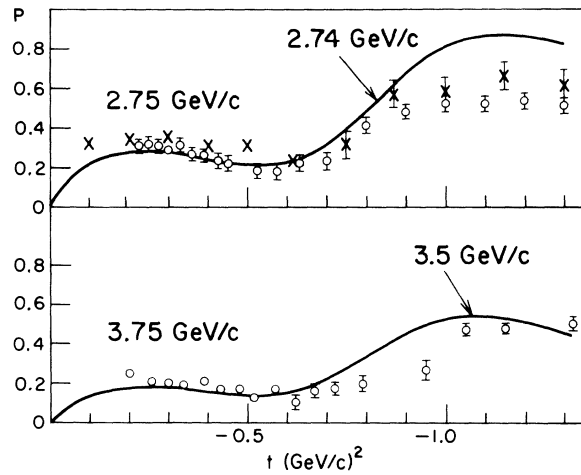


FIG. 2. Fits to the forward π^+p elastic-scattering polarization. Data from Ref. 5 (○) and Ref. 2 (×).

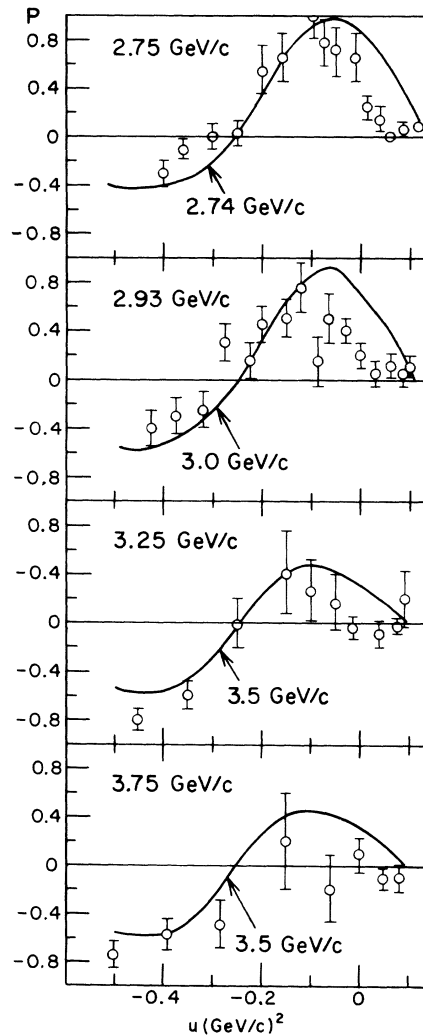


FIG. 3. Fits to the backward π^+p elastic-scattering polarization. Data from Ref. 5 (○).

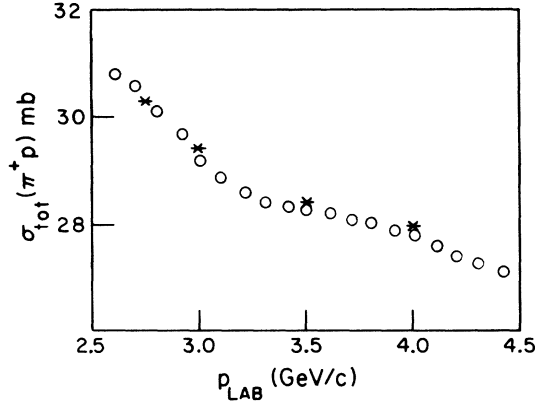


FIG. 4. Fits (*) to the π^+p total cross section. Data from Ref. 6 (O).

IV. FITS TO THE DATA; ANALYSIS OF OUR AMPLITUDES

Our fits to the differential cross sections at all angles for four energies (2.74, 3.0, 3.5, and 4.0 GeV/c) are presented in Fig. 1, the corresponding values of the parameters being given in Table I. In Figs. 2 and 3 we make comparisons with the available polarization measurements in the forward- and backward-scattering regions. Figure 4 shows our fits to the total π^+p cross sections. The total cross section, of course, restricts the imaginary part of the nonflip amplitude at $t=0$ through the optical theorem. In order to pin down also the real part of this amplitude at $t=0$, we used the results of Höhler and Strauss,¹³ who have calculated the real and imaginary parts of the πN nonflip amplitude at $t=0$ from forward dispersion relations; we constrained the real-to-imaginary ratio to give close agreement, as shown in Table II.

These fits seem sufficiently reasonable to provide substantial justification for the simple physical picture behind the parametrization. As far as we are aware, no other model (except, of course, the standard phase-shift analyses at much lower energies) has been able to correlate so much data throughout the whole scattering region in such a unified way, and this is the major achievement of the model.

We turn now to a more detailed analysis of our fits. As we shall show, the experimental features

TABLE II. Comparison of $\text{Re}f_{++}^s/\text{Im}f_{++}^s$ at $t=0$ with values obtained by Höhler and Strauss (Ref. 13) from forward dispersion relations.

| p_{lab} (GeV/c) | 2.74 | 3.0 | 3.5 | 4.0 |
|---|--------|--------|--------|--------|
| $\text{Re}f_{++}^s/\text{Im}f_{++}^s$ (Ref. 13) | -0.315 | -0.334 | -0.312 | -0.310 |
| $\text{Re}f_{++}^s/\text{Im}f_{++}^s$ | -0.31 | -0.33 | -0.31 | -0.31 |

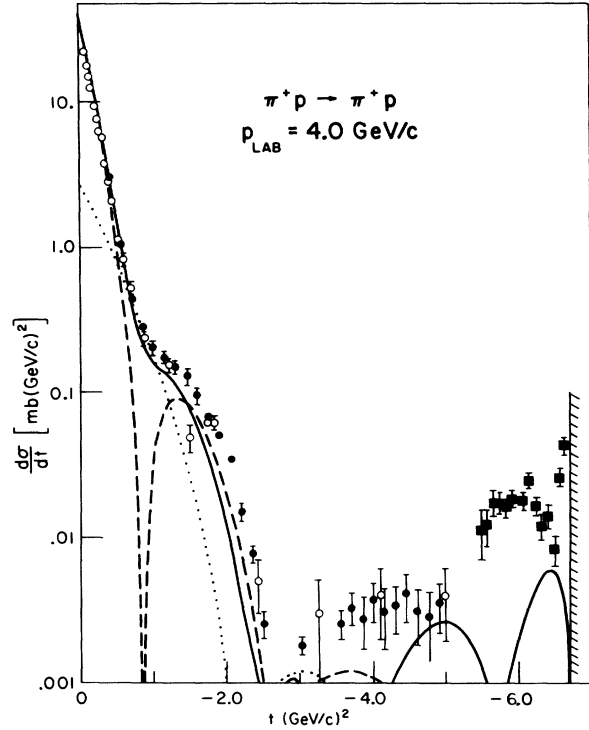


FIG. 5. Total contribution of the helicity-nonflip amplitude ($G_{++}^R + iG_{++}^I + BW_{++}$) to the differential cross section (solid line). We also indicate the contributions from G_{++}^R alone (dotted line) and G_{++}^I alone (dashed line).

come about in a natural way from the oscillations of the amplitudes. In order to avoid repetition, we shall concentrate on our fit to just one of the energies, namely 4.0 GeV/c; our fits to the other energies being similar.

A. Nonflip Amplitude

First of all, we show in Fig. 5 the contribution to the differential cross section from the s -channel helicity-nonflip amplitude, indicating also the separate contributions from G_{++}^R and iG_{++}^I . We see that the nonflip amplitude provides most of the differential cross section¹⁴ all the way out to about $t = -1.5$ (GeV/c)². The forward-diffraction peak arises primarily from the imaginary term iG_{++}^I , whose main contributions come from the *low* angular momentum states. To further illustrate this last point, we have drawn in Fig. 6 the shape of $\text{Im}T_{++}^j$ arising from iG_{++}^I alone [remember to divide out the $j + \frac{1}{2}$ factor on the left-hand side of Eq. (1)] as a function of j .

In all our fits, the break at $t \approx -0.85$ (GeV/c)² arises from the first (diffraction) zero of $\text{Im}f_{++}^s$; the hole there being filled up mainly by $\text{Re}f_{++}^s$. The real part of the nonflip amplitude, which is often ignored in many calculations (in spite of the fact that it is known¹³ to be about 30% of the imag-

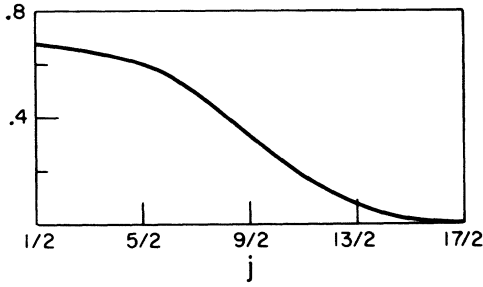


FIG. 6. Contribution to $\text{Im}T_{++}^j$ (expressed in dimensionless numbers) from iG_{++}^j as a function of j .

inary part at $t=0$), is therefore very important to us in our fitting scheme.

The role of the nonflip Breit-Wigner term is interesting. In contrast to the Gaussian terms, the Breit-Wigner term is centered around a higher angular momentum state with $j_c + \frac{1}{2} \approx 5.03$ (for 4.0 GeV/c). The former rapidly die away beyond $t = -2.8$ (GeV/c)², whereas the Breit-Wigner term pops up at large angles, helping in particular to fill the backward valley at $u = -0.2$ (GeV/c)².

B. Flip Amplitude

In Fig. 7, we have drawn the contributions from the s-channel helicity-flip amplitude, as well as

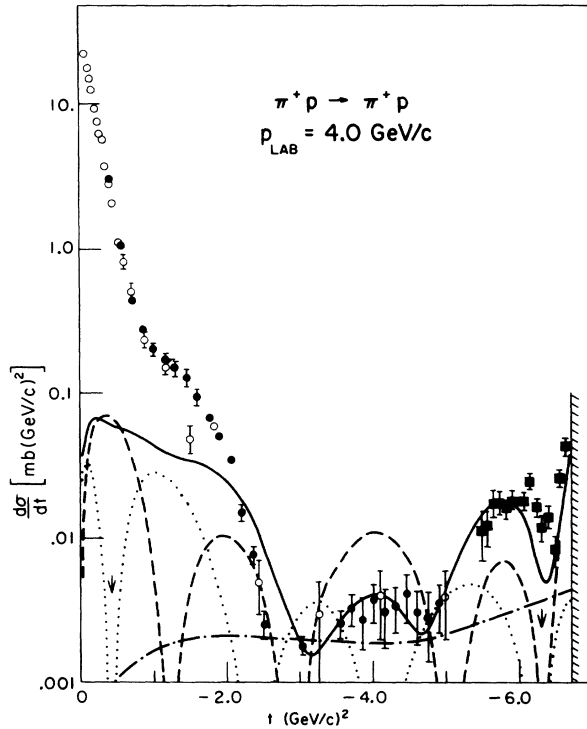


FIG. 7. Total contribution of the helicity-flip amplitude ($G_{+-}^R + iG_{+-}^I + \text{BW}_{+-}$) to the differential cross section (solid line). We also indicate the contributions from $G_{+-}^R + iG_{+-}^I$ (dash-dotted line), $\text{Re}(\text{BW}_{+-})$ (dotted line), and $\text{Im}(\text{BW}_{+-})$ (dashed line) separately.

the separate contributions from $\text{Re}(\text{BW}_{+-})$, $\text{Im}(\text{BW}_{+-})$, and $(G_{+-}^R + iG_{+-}^I)$. The flip amplitude clearly provides the dominant contribution at the larger angles, just as the nonflip amplitude dominated in the forward-scattering region, as discussed above. The oscillatory character is provided by the Breit-Wigner term. The width Γ of the angular momentum band is (see Table I) about 1.0, so the band is reasonably narrow; the oscillations correspondingly remain sizeable at all angles. In contrast, the Gaussian terms yield a featureless background (they contain only a few low angular momentum components). They assist mainly in damping out the vigorous oscillations of the flip Breit-Wigner term at the center of the scattering region where the differential cross section is exceedingly small.

One immediate test [see Sec. II, paragraph (ii)] of our ideas concerning the flip term is that the band of important angular momentum states described here by the Breit-Wigner term should move up in energy as the laboratory momentum increases, according to $j_c + \frac{1}{2} \approx kR$. In our fits to the data, we found (see Table I) that for $p_{\text{lab}} = 2.74, 3.0, 3.5,$ and 4.0 GeV/c, the corresponding values of $j_c + \frac{1}{2}$ were $j_c + \frac{1}{2} = 4.16, 4.31, 4.89,$ and 5.03 . Recalling that for these momenta $k = 1.05, 1.10, 1.20,$ and 1.30 GeV/c, respectively, we see that the energy dependence of j_c is indeed indicative of this relation, with the radius of interaction R taken as about $0.8 F \approx 4$ (GeV/c)⁻¹. The actual values of R for the various momenta are $0.80, 0.78, 0.81,$ and $0.78 F$, which are remarkably constant at around $0.8 F$.

C. Polarization

As a last comment on our fits, we mention how this model accounts for the observed features of the polarization near the forward and backward directions. One can easily see what happens by noting from Figs. 5 and 7 which are the dominant amplitudes in the various regions and where their zeros occur. The forward polarization arises primarily from the product of the dominant $\text{Im}f_{++}^s$ and the much smaller $\text{Re}f_{+-}^s$; the interesting dip at $t = -0.6$ (GeV/c)² in the polarization then arises from a zero in $\text{Re}f_{+-}^s$ at $t = -0.4$ (GeV/c)² and in $\text{Im}f_{++}^s$ at $t = -0.85$ (GeV/c)². The zero in the backward polarization at $u = -0.24$ (GeV/c)² arises from the zero in the dominant Breit-Wigner flip amplitude, which also causes the backward valley in the differential cross section at this position.

Even a cursory examination of the fits shows how the amplitudes are closely tied together. The smaller oscillations of an amplitude which may be dominant elsewhere can be crucially important in fitting the data, and there is not too much room

for leverage.

V. CONTRAST WITH REGGE MODELS

Those who are familiar with Regge-pole analyses^{7,8} will realize that the way the experimental structures are explained is considerably different for the two models. A detailed comparison of the models is presently under way; we shall therefore content ourselves here with a few brief remarks on some of the main differences between the Regge fits and our own fits (Sec. IV).

In the usual Regge fits,^{7,8} the imaginary Pomeranchuk contribution is *supposed* to represent diffraction. However, it is always parametrized as a smooth exponential in t , completely structureless (in both the t channel and s channel), with no zero at $t = -0.85$ (GeV/c)², as we have in our $\text{Im}f_{++}^s$.¹⁵ Furthermore, because the Pomeranchuk contribution is large,¹⁶ the choice for its parametrization substantially determines many other matters in the subsequent fitting. For example, the dip in the polarization at $t = -0.6$ (GeV/c)² is obtained in the Regge fits through the double zero of a no-compensation coupling for the P' , or through a nonsense wrong-signature zero from the ρ coupling together with a vanishing of the relative phase of the ρ and $P+P'$ contributions. These explanations illustrate what has been done if one chooses a smooth Pomeranchuk contribution.

There are differences also in the backward direction, where Regge fits^{8,9} rely on structure in the A and B amplitudes arising either from a nonsense wrong-signature zero of the nucleon coupling or from cuts. The s -channel helicity-flip amplitude, which dominates in the backward direction, actually goes over to the A' amplitude there (and not to A or B). It is therefore our A' which is most directly associated with the experimental data and gives rise to the observed features.

Our model also differs from the one recently proposed by Harari.¹⁷ He likewise bases his arguments on a smooth imaginary Pomeranchuk contribution, this assumption being taken from the smoothness of the differential cross section for elastic proton-proton scattering. Structures in differential cross sections, such as are observed in π^+p scattering at $t = -0.85$ (GeV/c)², then come about from destructive interference with s -channel resonances. However, as is evidenced by the strong shrinkage of the forward peak, the effective trajectory¹⁸ for $|t| < 2.0$ (GeV/c)² obtained from the elastic pp differential cross section in the intermediate energy region has a steep slope, about 1 (GeV/c)⁻², in contrast to the flat slope usually associated with the Pomeranchuk trajectory. Also, even though the pp differential cross sections are smooth at lower energies, they begin to develop

structure at $t = -0.85$ (GeV/c)² above 10 GeV/c, a well-defined shoulder¹⁹ being clearly visible at 20 GeV/c. This trend seems to run counter to the idea of a smooth Pomeranchuk contribution, which should presumably become the more dominant the higher the energy. Again, Harari's smooth Pomeranchuk contribution necessitates a double zero in one of his amplitudes (Ref_{+-}^s) to accommodate the π^+p polarization dip at $t = -0.6$ (GeV/c)².

VI. ENERGY DEPENDENCE AND CONCLUDING REMARKS

To understand the energy dependence of our fits, it is important to ask the question, "What is energy-independent?"

So far, we have been able to find three things that do not change much in the energy region we have investigated:

(i) In Fig. 8(a), we have drawn a graph of the contribution of iG_{++}^I to $\text{Im}T_{++}^j$ as a function not of j but of the *impact parameter* $b = (j + \frac{1}{2})/k$ for the four energies considered. We see that the shape²⁰ is more or less the same for all the energies. The graph indicates that absorption is substantial for low b , but rapidly decreases around a radius of

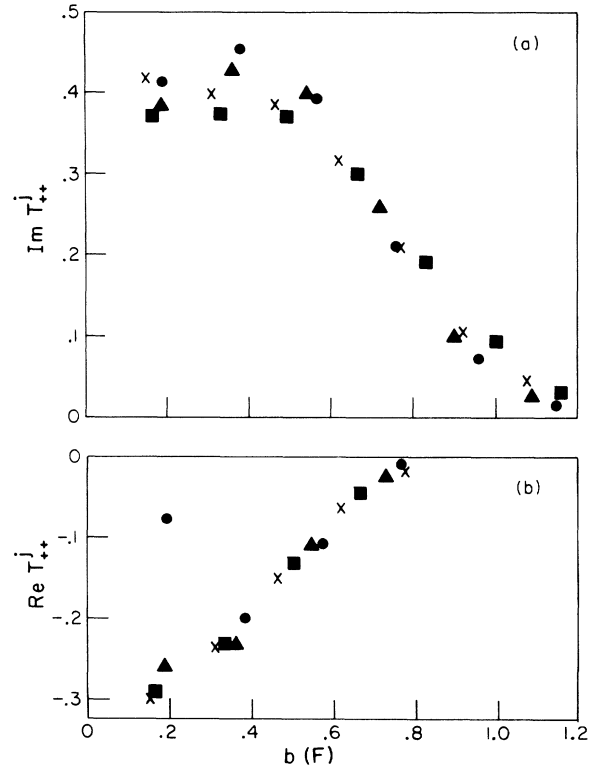


FIG. 8. (a) Graph of the contribution of iG_{++}^I to $\text{Im}T_{++}^j$ $\sqrt{\text{mb}}$ GeV as a function of the impact parameter b (in fermis) for the momenta 2.74 (●), 3.0 (▲), 3.5 (■), and 4.0 (×) GeV/c. (b) Graph of contribution of G_{++}^R to $\text{Re}T_{++}^j$ $\sqrt{\text{mb}}$ GeV as a function of b (in fermis); same convention as in (a).

about 0.8 F.

(ii) In Fig. 8(b), there is a similar graph of the contribution of G_{++}^R to $\text{Re}T_{++}^j$ for the four energies. Apart for one point, the shape again seems to be the same for all the energies.

(iii) The third energy-independent feature has already been mentioned in Sec. IV, where we remarked that the Breit-Wigner j -pole position increased with energy in a manner consistent with scattering from the edge of an object whose radius remains approximately constant at 0.8 F. It is important to realize from point (i) above that this is exactly the *same* radius where the absorption is rapidly decreasing.

Our conclusion therefore is that all the $\pi^+ p$ data we have fitted are consistent with the picture of scattering from an interaction region which is strongly absorbing out to a radius of about 0.8 F, at which range substantial edge effects (in the form of resonances) are important.

Since the main experimental features we have been discussing [forward-diffraction peak and backward peak with a valley at $u = -0.2$ (GeV/c)²]

occur at higher energies without any *new* type of feature appearing, one might speculate that *all* the data we have at present on $\pi^+ p$ elastic scattering are describable essentially in terms of the above physical picture. In one sense, it would of course be good to know that such a simple description is applicable; in another, it would be disappointing since it would mean that we have learned little about the deeper nature of the interaction itself. The dynamics are (still) wrapped up in exactly what is causing the internal absorption and the edge effects.

We are at present examining other processes (such as $\pi^- p$, CEX, and pp) to see if our model applies equally well in these situations. Our preliminary results indicate that this is indeed the case.

ACKNOWLEDGMENTS

We would like to acknowledge useful discussions with Professor R. G. Newton and Professor R. M. Weiner. We also wish to thank the Indiana University spark-chamber group for discussions and for supplying us with their data (Ref. 1).

*Supported in part by the Atomic Energy Commission under Contract No. AT(11-1)-2009, and by the National Science Foundation.

¹B. B. Brabson, R. R. Crittenden, R. M. Heinz, R. C. Kammerud, H. A. Neal, H. W. Paik, and R. A. Sidwell, Phys. Rev. Letters **25**, 553 (1970); J. P. Chandler, R. R. Crittenden, K. F. Galloway, R. M. Heinz, H. A. Neal, K. A. Potocki, W. F. Prickett, and R. A. Sidwell, *ibid.* **23**, 186 (1969).

²S. Andersson, C. Daum, F. C. Erne, J. P. Lagnaux, J. C. Sens, C. Schmid, and F. Udo, in *High Energy Collisions*, Third International Conference held at State University of New York, Stony Brook, 1969, edited by C. N. Yang, J. A. Cole, M. Good, R. Hwa, and J. Lee-Franzini (Gordon and Breach, New York, 1969).

³C. T. Coffin, N. Dikmen, L. Ettliger, D. Meyer, A. Saulys, K. Terwilliger, and D. Williams, Phys. Rev. **159**, 1169 (1967).

⁴D. R. Rust, P. N. Kirk, L. A. Lundy, C. E. W. Word, D. D. Yavanovitch, S. M. Pruss, C. W. Akerlof, K. S. Han, D. I. Meyer, and P. Schmuesser, Phys. Rev. Letters **24**, 1361 (1970).

⁵D. J. Sherden, N. E. Booth, G. Conforto, R. J. Esterling, J. Parry, J. Scheid, and A. Yokosawa, in *High Energy Collisions*, edited by C. N. Yang, J. A. Cole, M. Good, R. Hwa, and J. Lee-Franzini, Ref. 2; and Phys. Rev. Letters **25**, 898 (1970).

⁶A. Citron, W. Galbraith, T. F. Kycia, B. A. Leontic, R. H. Phillips, A. Rousset, and P. H. Sharp, Phys. Rev. **144**, 1101 (1966).

⁷For Regge fits to forward $\pi^+ p$ elastic scattering, see, for example, C. B. Chiu, S. Y. Chu, and L. L. Wang, Phys. Rev. **161**, 1563 (1967); W. Rarita, R. J. Riddell, C. B. Chiu, and R. J. N. Phillips, *ibid.* **165**, 1615 (1968); V. Barger and R. J. N. Phillips, *ibid.* **187**, 2210 (1969).

⁸For Regge fits to backward $\pi^+ p$ elastic scattering, see, for example, V. Barger and D. Cline, Phys. Rev. Letters **21**, 392 (1968); **21**, 1132(E) (1968); E. L. Berger and G. C. Fox, Nucl. Phys. **B26**, 1 (1971).

⁹F. Henyey, G. L. Kane, J. Pumplin, and M. H. Ross, Phys. Rev. **182**, 1579 (1969); R. L. Kelley, G. L. Kane, and F. Henyey, Phys. Rev. Letters **24**, 1511 (1970).

¹⁰P. Bareyre, C. Bricman, and G. Villet, Phys. Rev. **165**, 1730 (1968); A. T. Davies, Nucl. Phys. **B21**, 359 (1970); A. Donnachie, R. G. Kirsopp, and C. Lovelace, Phys. Letters **26B**, 161 (1968); C. H. Johnson, Jr., LRL Report No. UCRL-17683, 1967 (unpublished). A further extension of phase-shift methods has recently been suggested by D. Bridges, M. J. Moravcsik, and A. Yokosawa, Phys. Rev. Letters **25**, 771 (1970).

¹¹S. Y. Chu and A. W. Hendry, Phys. Rev. Letters **25**, 313 (1970). This paper contains references to previous optical and absorptive models.

¹²M. Jacob and G. C. Wick, Ann. Phys. (N.Y.) **1**, 404 (1959).

¹³G. Höhler and R. Strauss, University of Karlsruhe report, 1970 (unpublished).

¹⁴This goes somewhat further (at least for *pure elastic* scattering) than F. J. Gilman, J. Pumplin, A. Schwimmer, and L. Stodolsky [Phys. Letters **31B**, 387 (1970)], who, from Regge asymptotic considerations, have suggested "s-channel helicity conservation" near the forward scattering direction. We do not wish to suggest, however, that f_{++}^s necessarily dominates to such an extent in inelastic processes, or even in diffractionlike (but nonetheless *inelastic*) processes where, in Regge language, a Pomeron can be exchanged in the t channel.

¹⁵We have examined the phase-shift analyses for $1.0 \leq p_{lab} \leq 2.1$ GeV/c (Ref. 10) to see what information

they might provide on this point. No meaningful conclusion can be drawn at this stage, however. $\text{Im } f_{+}^s$ is strongly dependent on its $j = \frac{1}{2}$ components, but these low partial waves S_{31} and P_{31} are precisely the ones which are rather poorly determined at these momenta. (Likewise, in the $I = \frac{1}{2}$ state, it is the $j = \frac{1}{2}$ S_{11} and P_{11} waves which have the greatest notoriety among phase shifts.)

¹⁶Actually the P' contribution to the forward differential cross section and to the total cross section is just as large as the Pomeranchuk contribution in these fits, a fact that does not seem to have been made sufficiently clear before.

¹⁷H. Harari, *Ann. Phys. (N.Y.)* **63**, 432 (1971).

¹⁸R. C. Kammerud, B. B. Brabson, R. R. Crittenden, R. M. Heinz, H. A. Neal, H. W. Paik, and R. A. Sidwell, *Phys. Rev. D* **4**, 1309 (1971).

¹⁹J. V. Allaby, F. Binon, A. N. Diddens, P. Duteil, A. Klovning, R. Meunier, J. P. Peigneux, E. J. Sacharidis, K. Schlüpmann, M. Spighele, J. P. Stroot, A. M. Thorndike, and A. M. Wetherell, *Phys. Letters* **28B**, 67 (1968).

²⁰The shape resembles the well-known shape of the charge distribution inside a proton. It is not inconceivable that the two are related.

PHYSICAL REVIEW D

VOLUME 4, NUMBER 9

1 NOVEMBER 1971

Interpolation of the Energy Dependence of Partial-Wave Amplitudes*

R. E. Cutkosky and C. C. Shih †

Physics Department, Carnegie-Mellon University, Pittsburgh, Pennsylvania 15213

(Received 22 July 1971)

Two methods are described for interpolating the energy dependence of phase shifts. Both methods are based on normed analytic approximation theory. The first method interpolates the D function of the N/D method; the second interpolates the logarithm of this function. As an illustration, the methods are applied to the 1S_0 and 1P_1 n - p phase shifts below 400 MeV.

I. INTRODUCTION

This paper is devoted to a first exploratory attempt to apply the concepts of modern analytic interpolation theory^{1,2} to the problem of describing the energy dependence of phase shifts obtained from analysis of scattering data. By formulating new methods of analysis based on approximation theory, we may expect to obtain both a greater economy of parametrization and a more rigorous accounting for the effects of experimental uncertainties. To illustrate our method, we begin, in this first paper, by discussing a problem (n - p scattering) where there is no great controversy about the general trend of the phase shifts. Our aim is to explain our procedures by showing how they can be used to fit the phase shifts obtained by MacGregor *et al.*³ (the results of other groups⁴ are similar). In particular, we shall show that our interpolation formulas, with fewer parameters, can reproduce the given phase shifts within a reasonable tolerance, thus showing the greater efficiency of the parametrization suggested by analytic approximation theory.

Techniques based on the theory of approximation have been developed already for use in connection with partial-wave analyses (at a fixed energy), finite-energy sum rules, representation of form

factors, and related miscellaneous topics,⁵⁻¹³ and the value of these techniques has been demonstrated in several practical applications.¹⁴⁻¹⁶ Although we are able to make extensive use of the concepts and techniques already developed, the parametrization of the energy dependence of partial-wave amplitudes is a more complicated problem, for several reasons: (1) The analyticity information refers to a domain of meromorphy, rather than to a domain of holomorphy. (2) The unitarity relation ought to be treated exactly, which can be done most conveniently by linearizing it, at the cost of nonlinearizing either the relation to the data, or the relation to input ("left-hand") discontinuities. (3) It is necessary to make use of second-sheet analyticity and boundedness properties, which are not only more conjectural, but require use of more intricate conformal mappings. (4) With the exception of thresholds for opening of two-particle channels, the nature of even the branch points which lie in the physical region is not fully known; furthermore, there is always an enormous number of these, too many to treat explicitly. The first two points merely involve unpleasant technical complications, but the second two will also lead, unavoidably, to some residual model dependence in practical applications. It is important to try to find simple ways to overcome these diffi-